Pulse-width dependence of cooling effect on submicrometer ZnO spherical particle formation by pulsed laser melting in liquid

Shota Sakaki,*[a] Hiroshi Ikenoue,[b] Takeshi Tsuji,[c] Yoshie Ishikawa, [d] and Naoto Koshizaki[a]

Abstract: Submicrometer spherical particles can be synthesized by irradiating particles in liquid with a pulsed laser (pulse width: 10 ns). In this method, all of the laser energy is supposed to be spent for particle heating because nanosecond heating is far faster than particle cooling. To study the cooling effect, we fabricated submicrometer spherical particles using a pulsed laser with longer pulse widths (50 and 70 ns). From the increase in the laser–fluence threshold for submicrometer spherical particle formation with increasing pulse width, it is concluded that the particles dissipate heat to the surrounding liquid, even during several tens of nanoseconds of heating. A particle heating–cooling model considering the cooling effect is developed to estimate the particle temperature during laser irradiation. This model suggests that the liquid surrounding the particles evaporates, and the generated vapor films suppress heat dissipation from the particles, resulting in efficient heating and melting of the particles in the liquid. In the case of small particle sizes and large pulse widths, the particles dissipate heat to the liquid without forming such vapor films.

1. Introduction

Over the past few decades, nanoparticle fabrication by pulsed laser irradiation with high fluence targeting material immersed in liquid (pulsed laser ablation in liquid) has been widely studied.[1-5] In this method, nanoparticles are generated by an explosive interaction between bulk material and high-power laser light.

Recently, the synthesis of submicrometer spherical particles by irradiating particles dispersed in liquid with a nanosecond pulsed laser was reported.[6] Particles dispersed in liquid are instantaneously heated over the melting point of the material when particles have adequate optical absorption of nanosecond pulsed laser light, whereas the dispersion medium is barely heated due to its optical transparency. The molten droplets are then quenched by the unheated surrounding liquid, maintaining the spherical shape of the droplets.[6-9] The droplets of raw particles merge with adjacent droplets, which results in the growth of submicrometer spherical particles.[10, 11] Through this rapid particle heating and cooling, submicrometer spherical particles are formed. This technique has been successfully applied to various materials including metals, semiconductors, and oxides (e.g., Au, Ag, Si, ZnO, and TiO_2).[7, 8, 12,-14]

Pyatenko et al. developed a particle heating–melting–evaporation model that well explains the spherical particle formation conditions.[11, 15, 16] In this model, all of the laser energy absorbed by a particle is assumed to be exclusively utilized for particle heating. A laser–fluence curve as a function of particle size for the phase transition from solid to liquid can then be obtained. This curve is quite useful to explain the submicrometer spherical particle formation mechanism and to predict the laser fluence required to obtain submicrometer spherical particles. The curve with a positive slope in the size range of several hundreds of nanometers suggests that the particle size increases with laser fluence.

The particle heating-melting-evaporation model considered particle cooling only by boiling conductive/convective heat transfer. This cooling rate is slow comparting with particle heating, and therefore cooling process was ignored in this model. However, heat dissipation by the liquid-phase surroundings is possibly considerable. Heated particles would be rapidly cooled by the liquid medium in the initial heating stage by laser pulse, and then heat dissipation from particles is disturbed by the vapor-phase surroundings generated by evaporation of surrounding liquid medium in the subsequent heating stage. We fabricated submicrometer spherical particles using a nanosecond pulsed laser with different pulse widths of 50 and 70 ns to study the pulse width effect on the products. If the laser fluence of a single laser pulse is the same, the pulse width should not affect submicrometer spherical particle formation according to the particle heating–melting–evaporation model without considering cooling effects of liquid-phase surroundings. However, in our experiments, the laser–fluence threshold for submicrometer spherical particle formation increased as the pulse width increased, which suggests the contribution of a cooling process during pulsed laser heating. Here we propose a new particle heating–cooling model to explain this experimental result. Based on this new model, we also calculate time-dependent profiles of particle temperature, and computationally clarify the pulse-width dependence of the cooling effect. The calculation results are compared with experimental results to verify the validity of the developed particle heating–cooling model.

[a] *S. Sakaki, Prof. Dr. N. Koshizaki*
Division of Quantum Science and Engineering
Graduate school of Engineering
Hokkaido University
Kita 13, Nishi 8, Kita-ku, Sapporo, Hokkaido 060-8628 (Japan)
E-mail: sakaki.shota@frontier.hokudai.ac.jp
koshizaki.naoto@eng.hokudai.ac.jp
[b] *Prof. Dr. H. Ikenoue*
Department of Gigaphoton Next GLP
Graduate School of Information Science and Electrical Engineering
Kyushu University
744 Motooka, Nishi-ku, Fukuoka 819-0395 (Japan)
[c] *Prof. Dr. T. Tsuji*
Interdisciplinary Graduate School of Science and Engineering, Chemistry
Shimane University
1060 Nishikawatsu-cho, Matsue, Shimane 690-8504 (Japan)
[d] *Dr. Y. Ishikawa*
Nanomaterials Research Institute, National Institute of Advanced Industrial Science and Technology (AIST)
Tsukuba Central 5, 1-1-1 Higashi, Tsukuba, Ibaraki 305-8565 (Japan)

2. Results and Discussion

2.1. Experimental results

In this study, colloidal ZnO particles were irradiated with a KrF excimer laser (Gigaphoton Inc., wavelength 248 nm, pulse frequency 100 Hz, pulse width 50 or 70 ns) (Figure 1). Commercial ZnO powder (Sigma-Aldrich Co., LLC) was dispersed in de-ionized water with a ZnO concentration of 0.2 mg/ml. Then, 6 ml of the suspension in a glass vessel was irradiated for 8 min at various laser fluences with agitation by a magnetic stirrer. The laser beam was focused using a lens with a focal length of 500 mm to adjust the laser fluence (beam size 1.5 mm × 8.7 mm square). Part of the particles in suspension absorb laser energy and melt. By repeating this process with agitation for sufficient time, submicrometer spherical particles with homogeneous size distribution are formed.[9] The quenching process is usually reported to require 10^{-6} to 10^{-4} s.[17-21] This quenching time is much shorter than the interval between two consecutive laser pulses in this experiment. Therefore, no heat energy from a laser pulse is retained in the particle just before the subsequent laser pulse arrives, and particles can be regarded as independently interacting with each laser pulse. The suspension after laser irradiation was settled for a day to separate insufficiently treated raw particles and nanoparticle by-products from the produced submicrometer spherical particles. The precipitation in the glass vessel was dropped onto a Si substrate to observe the particle morphology using a field-emission scanning electron microscope (FE-SEM).

SEM images of raw ZnO particles and particles obtained by KrF excimer laser irradiation with different pulse widths at 81 mJ pulse^{-1} cm^{-2} are presented in Figures 2(a), (b), and (c). Raw particles have non-spherical shapes with an average diameter of about 60 nm (Figure 2(a)). At a pulse width of 50 ns, agglomerates of raw particles were melted, and submicrometer spherical particles with an average diameter of about 170 nm were formed (Figure 2(b)). In contrast, at a pulse width of 70 ns, particles after laser irradiation were not spherical and were almost identical to the raw particles (Figure 2(c)), though 81 mJ pulse^{-1} cm^{-2} is a sufficient laser fluence for agglomerates to melt based on the estimation by the particle heating–melting–evaporation model ignoring the pulse width effect. Pulsed lasers with short pulse widths would be efficient for pulsed laser melting in liquid because heating by longer pulses is supposed to cause larger heat dissipation.

Figures 3(a) and (c) present the SEM images of the particles obtained after KrF excimer laser irradiation with different pulse widths at a larger laser fluence of 202 mJ pulse^{-1} cm^{-2}. For both pulse widths of 50 and 70 ns, submicrometer spherical particles were obtained. Additionally, the average size distribution histograms plotted by counting more than 200 particles are almost identical, regardless of pulse width (Figures 3 (b) and (d)). At high laser fluence, the pulse width has little influence on the products obtained by pulsed laser melting in liquid.

The laser–fluence dependence of the average diameter and standard deviation of the obtained ZnO particles calculated from the SEM images are depicted in Figure 4. The average diameter increases with laser fluence when the laser fluence exceeds the threshold for submicrometer spherical particle formation. In addition, the laser–fluence threshold increases with increasing pulse width. For the case of a KrF excimer laser with a pulse width of 50 ns, a laser fluence of 81 mJ pulse^{-1} cm^{-2} was the threshold, whereas a laser fluence of 101 mJ pulse^{-1} cm^{-2} was required for 70 ns. When the third harmonic of an Nd:YAG laser with a pulse width of 10 ns is used, the laser–fluence threshold is 67 mJ pulse^{-1} cm^{-2},[8] which is smaller than for the KrF excimer laser with pulse widths of 50 and 70 ns. The amount of laser energy absorbed by a particle from one pulse is almost the same regardless of the pulse width. This result suggests that the particles dissipate heat energy to the surrounding liquid during pulsed laser heating and the maximum heat energy accumulated in the particles decreases with increasing pulse width.

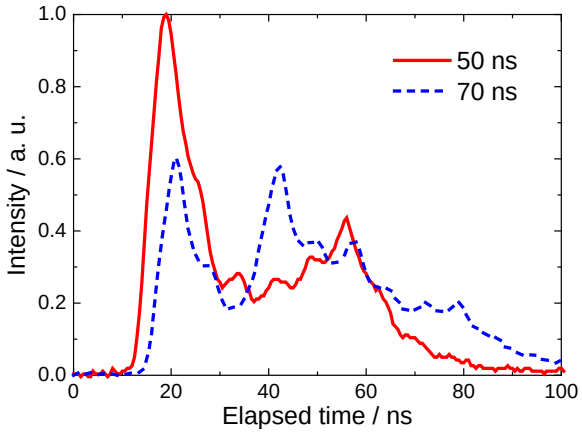

Figure 1. Temporal pulse profile of a KrF excimer laser with a pulse width of 50 ns (red solid curve) or 70 ns (blue dashed curve).

2.2. Particle heating–cooling model

The particle heating–melting–evaporation model could explain well the submicrometer spherical particle formation in our previous studies using a 10 ns pulse width Nd:YAG laser.[11, 16] However, particle cooling by the surrounding liquid, which might affect submicrometer spherical particle formation, was not considered to be significant in these studies. Here we take the cooling process into consideration and develop a new particle heating–cooling model describing the submicrometer spherical particle formation process. In this model, a homogeneous distribution of heat energy within a spherical particle and no volume change of the spherical particle during heating and cooling are assumed. The time required for submicrometer spherical particles to cool to room temperature is much shorter than 10 ms.[17-21] The calculations have been performed for a single pulse, because the pulse repetition rate of the laser used in these experiments is 100 Hz (pulse interval: 10 ms).

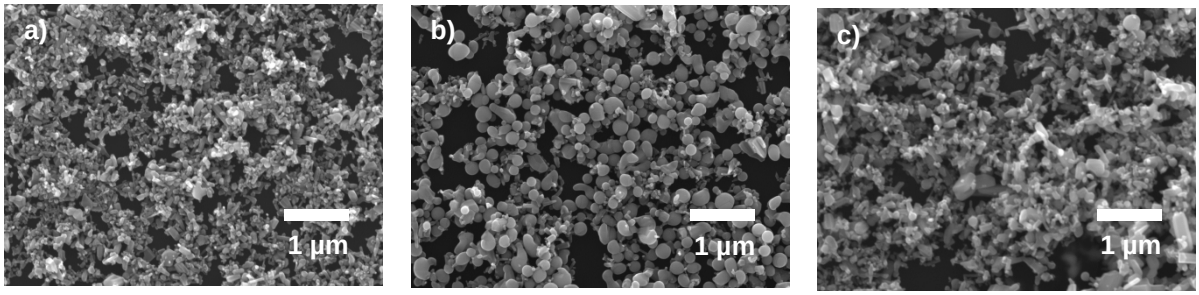

Figure 2. SEM images of ZnO particles. Raw particles (a) and after KrF excimer laser irradiation at a laser fluence of 81 mJ pulse^{-1} cm^{-2} with a pulse width of 50 ns (b) or 70 ns (c).

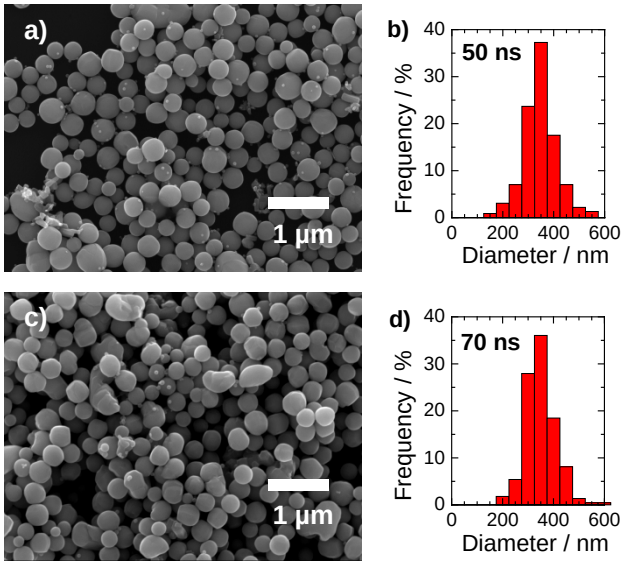

Figure 3. SEM images of ZnO particles after KrF excimer laser irradiation at a laser fluence of 202 mJ pulse^{-1} cm^{-2} with a pulse width of (a) 50 ns or (c) 70 ns. The corresponding particle size distributions from (a) and (c) are shown in (b) and (d), and the average particle sizes are 327 nm and 323 nm, respectively.

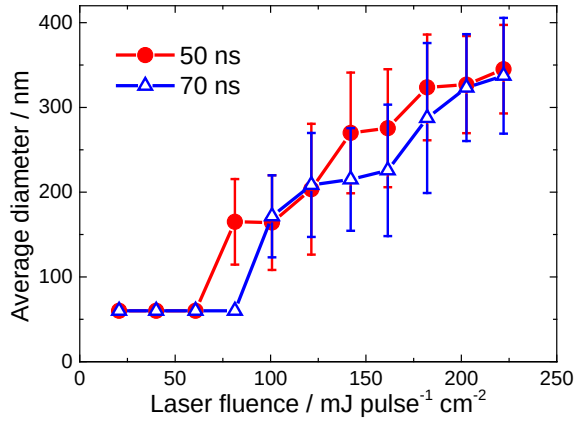

Figure 4. Laser-fluence dependence of average particle diameter of ZnO particles obtained by nanosecond pulsed KrF excimer laser irradiation with a pulse width of 50 ns (red circles) or 70 ns (blue triangles).

2.2.1. Particle heating

Particles absorb laser energy depending on the pulse shape of the laser. In this model, all laser energy absorbed by the particle is converted to particle heat energy.

$$\frac{dE_{abs}}{dt} = Q_{abs}^{\lambda} \cdot \frac{\pi d^2}{4} \cdot J(t) \quad (1)$$

Here, Q_{abs}^{λ} is the absorption efficiency based on Mie theory, $\frac{\pi d^2}{4}$ is the particle geometrical cross section, and $J(t)$ is the time-dependent laser fluence. The integral of time-dependent laser fluence corresponds to the laser fluence.

2.2.2. Particle cooling

The heat energy of the particles diffuses to the surrounding liquid. In this model, conductive heat transfer is defined because convection around submicrometer-scale particle is neglligible.[22]

$$\frac{dq}{dt} = h \cdot \pi d^2 \cdot \{T(t) - T_0\} \quad (2)$$

where

$$h = \frac{Nu_d \cdot k_w}{d} \quad (3)$$

Here, h is the heat transfer coefficient, πd^2 is the particle surface area, $T(t)$ is the particle temperature, and T_0 is the temperature of the surrounding liquid. The heat transfer coefficient is proportional to the heat conductivity of the surrounding liquid, k_w, Nusselt number, Nu_d, and inversely proportional to the particle diameter, d. In the case of submicrometer particles in water, heat transfer coefficient can be estimated 1.2 to 12 MW m^{-2} K^{-1}. This value is much larger than the value estimated in heating-melting-evaporation model. Therefore, cooling process have influence on heat dissipation of particles.

In the initial heating stage, particles contact directly with the liquid and are cooled. At the spinodal temperature of 573 K, explosive evaporation of the water is reported to occur,[23-25] and heated particles start to be cooled by vaporized liquid over 573 K with the following heat transfer coefficient value.

$$h = \frac{Nu_d \cdot k_v}{d} \quad (4)$$

Here, k_v is the heat conductivity of the surrounding evaporating vapor. The heat conductivity of vapor is much lower than that of liquid and, therefore, the cooling rate by vapor is much slower than by liquid. Cooling process is drastically switched by evaporation of surrounding liquid.

The Nusselt number is the ratio of convective heat transfer to conductive heat transfer. In the case of natural convection on a sphere, the Nusselt number is given as below.[26]

$$\overline{Nu_d} = 2 + \frac{0.589 Ra_d^{1/4}}{\left[1 + (0.469/Pr)^{9/16}\right]^{4/9}} \quad (5)$$

Here, Ra_d is the Rayleigh number and Pr is the Prandtl number. In submicrometer scale heating, heat transfer is governed by heat conduction but not by fluid convection. In this case, the Nusselt number is constant, $Nu_d \approx 2$, because the Rayleigh number is negligibly small on the submicrometer scale.[22]

Thermal particle-water interface resistance is considered in the case of Au nanoparticles irradiated with femtosecond, picosecond and nanosecond lasers.[27, 28] However, conductive heat transfer does not contain interfacial condition, and the step of temperature across the interface of particle and liquid is in quasi-equilibrium for the nanosecond case.[29] Therefore, we considered the step of temperature would be negligible during several tens of nanosecond heating.

2.2.3. Time-dependent particle temperature

The accumulated heat energy in a particle is the difference between the laser energy absorbed by a particle and the energy dissipated by conductive heat transfer.

$$\frac{dE}{dt} = \frac{dE_{abs}}{dt} - \frac{dq}{dt} \quad (6)$$

If the laser energy is not enough to melt the agglomerate of raw particles, only particle heating in the solid state is expected.

$$T(t) = T_0 + \frac{1}{\rho_p \frac{\pi d^3}{6} c_s} \cdot E(t) \quad (7)$$

Here, ρ_p is the density of the particle, $\frac{\pi d^3}{6}$ is the particle volume, and c_s is the particle specific heat in the solid state.

If the agglomerate absorbs more energy, particle melting occurs.

$$T(t) = T_m \quad (8)$$

Here, T_m is the melting point of the material. During particle melting, the particle temperature stays at the melting point.

With more absorbed energy, the particle completely melts and the temperature of the droplet increases further.

$$T(t) = T_{\mathrm{m}} + \frac{1}{\rho_p \frac{\pi d^3}{6} c_l} \cdot \left[E(t) - \rho_p \cdot \frac{\pi d^3}{6} \cdot \left(H_{T_m} - H_{T_0} + \Delta H_m\right)\right] \quad (9)$$

Here, $H_{T_m} - H_{T_0}$ is the relative enthalpy required for start of melting, ΔH_m is the latent enthalpy of melting, and c_l is the particle specific heat in the liquid state.

2.3. Temporal temperature profile

By numerically solving the differential equation using a fourth-order Runge–Kutta method, the time profile of the particle temperature of ZnO spherical particles can be calculated. The pulse shape of the time-dependent laser fluence used in the calculation is plotted in Figure 1. The optical data used in the calculation are listed in Table 1,[30] and all thermodynamic data are listed in Tables 2 and 3.[25, 31, 32] The absorption efficiency of ZnO spherical particles at a wavelength of 248 nm was calculated from refractive index and extinction coefficient using Mie theory (Figure 5).

Figure 6 depicts the calculated time-dependent temperature profile of ZnO spherical particles 60 nm in diameter irradiated with a KrF excimer laser (wavelength 248 nm, pulse width 50 or 70 ns) at laser fluences of 61, 81, and 101 mJ pulse^{-1} cm^{-2}. These laser fluences are sufficient for particle melting (dotted line: T_m) when the adiabatic condition is satisfied. The particle temperature calculated under the adiabatic condition (dashed line: T_{ad}) increased with increasing laser fluence. However, in this experiment, submicrometer spherical particles were formed from 81 mJ pulse^{-1} cm^{-2} for 50 ns pulse width and from 101 mJ pulse^{-1} cm^{-2} for 70 ns pulse width.

At a laser fluence of 61 mJ pulse^{-1} cm^{-2}, which is sufficient for particle melting under the adiabatic condition, the maximum particle temperature is below the melting point in both cases of 50 and 70 ns pulse widths (Figure 6(a)). For a 70 ns pulse width, the particle temperature is below the spinodal temperature of the surrounding water (chained line: T_{sp}), and the particles are rapidly cooled by liquid water. In contrast, for the 50 ns pulse width, the particle temperature is above the spinodal temperature and, therefore, the surrounding liquid evaporates and the generated vapor disturbs heat dissipation from the particles. Therefore, the particle temperature is much higher when irradiated with 50 ns pulses than with 70 ns pulses due to the lower heat loss of 50 ns pulses.

At a laser fluence of 81 mJ pulse^{-1} cm^{-2}, the particle temperature reaches the melting point of ZnO for a 50 ns pulse width, but is below the spinodal temperature for a 70 ns pulse width because heating rate is comparatively lower than cooling rate by water (Figure 6(b)). At a laser fluence of 101 mJ pulse^{-1} cm^{-2}, the particle temperature reaches the melting point of ZnO for 70 ns pulse widths (Figure 6(c)). Once particle temperature exceeds the spinodal temperature, attained temperature is drastically increased. These calculation results considering the cooling effect by the surrounding liquid are in good agreement with the experimental results on spherical particle formation. When the temperature of the raw particles reaches the melting point of the material, submicrometer spherical particles are formed. During nanosecond pulsed heating of submicrometer particles, the formation of vapor films around particles is essential for them to melt in liquid.

2.4. Fluence- and size-dependent maximum temperature

Figure 7 illustrates numerical calculation results of the maximum temperature of ZnO spherical particles irradiated with a KrF excimer laser. Under the adiabatic condition, no heat is

dissipated from the particles to the surrounding liquid during pulsed heating. The laser fluence required to attain the same temperature almost linearly increases with particle diameter for diameters above 100 nm and is nearly constant below 100 nm. A higher maximum temperature is attained when a larger fluence is applied (Figure 7(a)). By considering the cooling effect and the pulse width of the KrF excimer laser, the maximum temperature is decreased, especially for small particles and low laser fluence (Figures 7(b) and 7(c)). Thus, we find a clear dip in the fluence–size diagram, indicating that 100 nm particles can be selectively melted with smaller laser fluence. For large particles, the maximum temperature considering the cooling effect is almost the same as that under the adiabatic condition. The plotted circles and triangles in Figure 7 are the experimental results shown in Figure 4. Submicrometer spherical particles are formed in the region above the melting point of ZnO (gray-colored region). In contrast, raw particles are not melted and maintain their shape and size if they stay in the region below the melting point.

The region in black in Figure 7, which shows where the particle temperature is barely elevated, expands toward larger particle size with increasing pulse width. At a laser fluence of 150 mJ pulse^{-1} cm^{-2}, nanoparticles smaller than 40 nm or 50 nm are insufficiently heated for pulse widths of 50 ns or 70 ns, respectively (Figures 7(b) and 7(c)).

Table 1. Refractive index and extinction coefficient of zinc oxide at a wavelength of 248 nm.

	n	*k*
ZnO	1.808	0.509

Table 2. Thermodynamic data of water used in the calculations.

	T_0 K	$T_{spinodal}$ K	k_w (298 K) W/m · K	k_v (573 K) W/m · K
Water	298	573	0.61	0.043

Table 3. Thermodynamic data of zinc oxide used in the calculations.

	ρ g/cm^3	T_{melt} K	ΔH_m kJ/kg	$H_{T_m} - H_{T_0}$ kJ/kg	C_s kJ/kg · K	C_l kJ/kg · K
ZnO	5.606	2243	870.65	1284.37	0.660	0.757

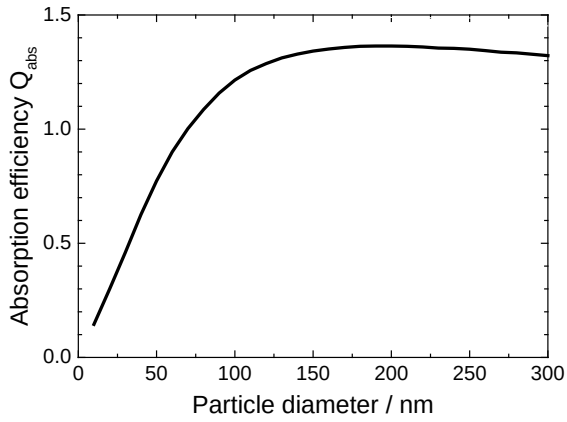

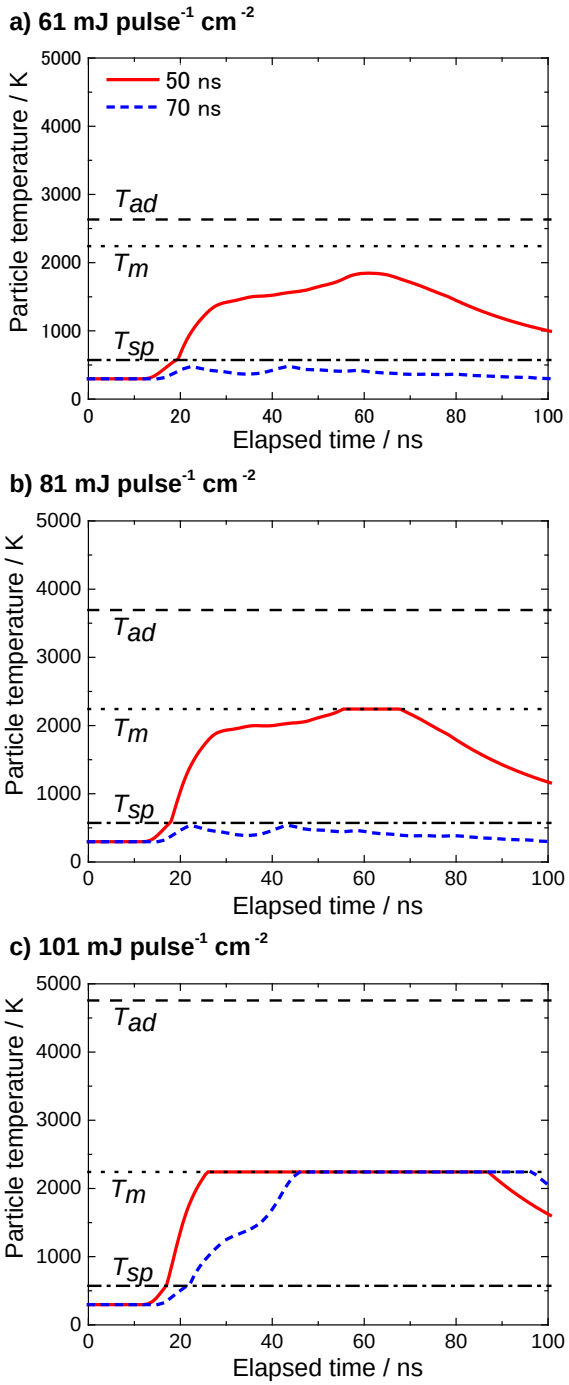

Figure. 5. Absorption efficiency of ZnO spherical particles at a wavelength of 248 nm calculated using Mie theory.

Figure. 6. Time-dependent temperature profile of ZnO particles 60 nm in diameter irradiated with a KrF excimer laser at laser fluences of 61 mJ pulse^{-1} cm^{-2} (a), 81 mJ pulse^{-1} cm^{-2} (b), and 101 mJ pulse^{-1} cm^{-2} (c). In each graph, temperature profiles calculated using the model considering the cooling effect are shown for pulse widths of 50 ns (red solid curve) and 70 ns (blue dashed curve). The dotted horizontal line represents the melting point of zinc oxide, T_m, the dashed horizontal line represents the particle temperature under the adiabatic condition, T_{ad}, and the chained horizontal line represents the spinodal temperature of water, T_{sp}.

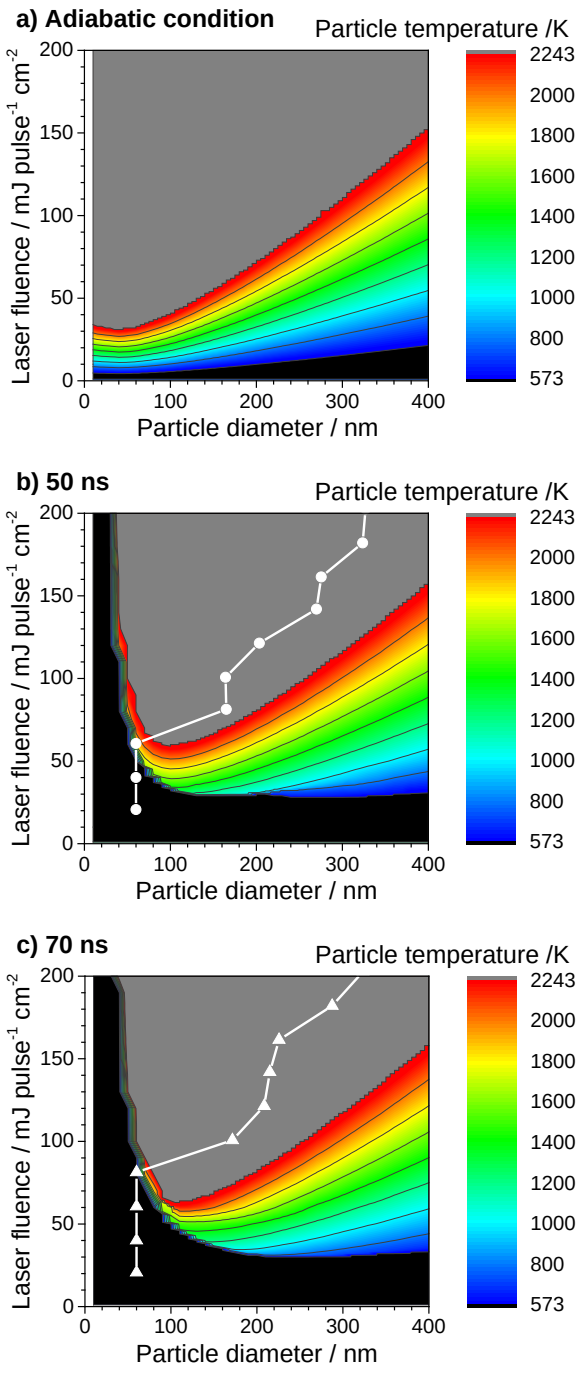

Figure 7. Two-dimensional diagram of the highest temperature attained as a function of laser fluence and particle size for ZnO spherical particles irradiated with KrF excimer laser (a) under the adiabatic condition, and based on a model considering the cooling effect with laser pulse widths of 50 ns (b) and 70 ns (c).

3. Conclusions

Submicrometer ZnO spherical particle formation by pulsed laser melting in liquid is examined using a nanosecond pulsed excimer laser with different pulse widths. The threshold fluence for submicrometer spherical particle formation increases with increasing pulse width from 50 to 70 ns. This result suggests that the particles dissipate heat energy even during several tens of nanoseconds pulsed heating, especially in the case of longer pulse widths with lower laser fluence. Considering the cooling effect of the surrounding liquid, a particle heating–cooling model is developed to estimate the particle temperature profile during nanosecond pulsed laser irradiation. Vapor films considered to be formed from the heated liquid surrounding the particles significantly suppress the heat dissipation from the particles to the liquid and elevate the maximum temperature attained. However, if the particle size is small or the pulse width is large, the transient temperature during heating is not high enough to form vapor films, resulting in a drastic lowering of the maximum temperature. Utilizing the heating–cooling model developed here, the threshold fluence for spherical particle formation and maximum particle temperature can be estimated, which is useful for predicting the fabrication conditions for submicrometer spherical particles.

Acknowledgements

This work was partially supported by JSPS KAKENHI Grant Number 26289266 and 26870908, and by The Ministry of Education, Culture, Sports, Science and Technology through the Program for Leading Graduate Schools (Hokkaido University Ambitious Leader's Program).

Keywords: nanoparticles • colloids • phase transitions • energy transfer • thermodynamics

[1] P. P. Patil, D. M. Phase, S. A. Kulkarni, S. V. Ghaisas, S. K. Kulkarni, S. M. Kanetkar, S. B. Ogale, V. G. Bhide, Phys. Rev. Lett. **1987**, 58, 238-241.

[2] J. Neddersen, G. Chumanov, T. M. Cotton, Appl. Spectrosc. **1993**, 47, 1959-1964.

[3] B. G. Ershov, E. Janata, A. Henglein, J. Phys. Chem. **1993**, 97, 339-343.

[4] F. Mafuné, J. Kohno, Y. Takeda, T. Kondow, J. Phys. Chem. B **2000**, 104, 9111-9117.

[5] C. Liang, Y. Shimizu, M. Masuda, T. Sasaki, N. Koshizaki, Chem. Mater. **2004**, 16, 963−965.

[6] Y. Ishikawa, Y. Shimizu, T. Sasaki, N. Koshizaki, Appl. Phys. Lett. **2007**, 91, 161110.

[7] H. Wang, M. Miyauchi, Y. Ishikawa, A. Pyatenko, N. Koshizaki, Y. Li, L. Li, X. Li, Y. Bando, D. Golberg, J. Am. Chem. Soc. **2011**, 133, 19102-19109.

[8] H. Wang, N. Koshizaki, L. Li, L. Jia, K. Kawaguchi, X. Li, A. Pyatenko, Z. Swiatkowska-Warkocka, Y. Bando, D. Golberg, Adv. Mater. **2011**, 23, 1865-1870.

[9] H. Wang, K. Kawaguchi, A. Pyatenko, X. Li, Z. Swiatkowska-Warkocka, Y. Katou, N. Koshizaki, Chem. Eur. J. **2012**, 18, 163-169.

[10] Y. Ishikawa, Y. Katou, N. Koshizaki, Q. Feng, Chem. Lett. **2013**, 42, 530-531.

[11] A. Pyatenko, H. Wang, N. Koshizaki, J. Phys. Chem. C **2014**, 118, 4495-4500.

[12] T. Tsuji, T. Yahata, M. Yasutomo, K. Igawa, M. Tsuji, Y. Ishikawa, N. Koshizaki, Phys. Chem. Chem. Phys. **2013**, 15, 3099-3107.

[13] X. Li, N. Koshizaki, A. Pyatenko, Y. Shimizu, H. Wang, J. Liu, X. Wang, M. Gao, Z. Wang, X. Zeng, Opt. Exp., **2011**, 19, 2847
[14] X. Li, A. Pyatenko, Y. Shimizu, H. Wang, K. Koga, N. Koshizaki, Langmuir, **2011**, 27, 5076-5080
[15] A. Pyatenko, H. Wang, N. Koshizaki, T. Tsuji, Laser Photon. Rev. **2013**, 7, 596-604.
[16] Y. Ishikawa, N. Koshizaki, A. Pyatenko, N. Saitoh, N. Yoshizawa, Y. Shimizu, J. Phys. Chem. C **2016**, 120, 2439-2446.
[17] A. Pyatenko, M. Yamaguchi, M. Suzuki, J. Phys. Chem. C **2007**, 111, 7910-7917.
[18] S. Link, M. El-Sayed, J. Phys. Chem. B **1999**, 103, 4212-4217.
[19] A. Takami, H. Kurita, S. Koda, J. Phys. Chem. B **1999**, 103, 1226-1232.
[20] P. V. Kamat, M. Flumiani, G. V. Hartland, J. Phys. Chem. B **1998**, 102, 3123-3128.
[21] A. Pyatenko, M. Yamaguchi, M. Suzuki, J. Phys. Chem. C **2009**, 113, 9078-9085.
[22] J. S. Donner, G. Baffou, D. McCloskey, R. Quidant, ACS Nano **2011**, 5, 5457-5462.
[23] F. Caupin, E. Herbert, C. R. Phys. **2006**, 7, 1000-1017
[24] V. Kotaidis, C. Dahmen, G. von Plessen, F. Springer, A. Plech, J. Chem. Phys. **2006**, 124, 184702
[25] A. Siems, S. A. L. Weber, J. Boneberg, A. Plech, New J. Phys. **2011**, 13, 043018.
[26] A. F. Mills, Heat Transfer 2nd edition, Prentice Hall, New York, **1998**, pp. 275-282.
[27] A. Plech, V. Kotaidis, Phys. Rev. B **2004**, 70, 195423.
[28] S. Hashimoto, D. Werner, T. Uwada, J. Photochem. Photobiol. C **2012**, 13, 28-54.
[29] D. Werner, S. Hashimoto, J. Phys. Chem. C **2011**, 115, 5063-5072.
[30] H. Yoshikawa, S. Adachi, Jpn. J. Appl. Phys. **1997**, 36, 6237-6243.
[31] Thermodynamic database MALT group, Thermodynamic database MALT for Windows, Kagaku Gijutsu-Sha, 2005, (CD-ROM), available from (http://www.kagaku.com/malt/index.html), (accessed 2016-10-20).
[32] http://www.chem.msu.su/Zn/Zn/ivtan0003.html, (in Russian, accessed 2016-10-20).

Entry for the Table of Contents (Please choose one layout)

Layout 1:

ARTICLE

Heat dissipation during nanosecond heating: When particles dispersed in liquid are irradiated with a pulsed laser (50–70 ns pulse width), the particles dissipate heat to the surrounding liquid, especially in the case of small particle sizes and large pulse widths. We can estimate the laser fluence for submicrometer spherical particle formation and the morphology of particles after laser irradiation by considering the cooling effect.

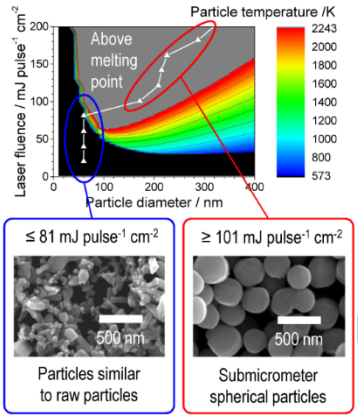

Shota Sakaki, Prof. Hiroshi Ikenoue, Prof. Takeshi Tsuji, Dr. Yoshie Ishikawa, Prof. Naoto Koshizaki

Page No. – Page No.

Pulse-width dependence of cooling effect on submicrometer ZnO spherical particle formation by pulsed laser melting in liquid